Aust. J. Phys., 1992, **45**, 221–38

Lattice Dynamics of $YBa_2Cu_3O_{6+x}$ ($x = 0, 1$)

K. K. Yim,[A] *J. Oitmaa*[A] *and M. M. Elcombe*[B]

[A] School of Physics, University of New South Wales, Kensington, N.S.W. 2033, Australia.
[B] Australian Nuclear Science and Technology Organisation, Menai, N.S.W. 2234, Australia.

Abstract

We report shell model based calculations of the lattice dynamics of $YBa_2Cu_3O_6$ and $YBa_2Cu_3O_7$. Two models are proposed for $YBa_2Cu_3O_6$, the model parameters being obtained by a least squares fit to recent neutron scattering results. The parameters obtained are then used, with modification, to model the lattice dynamics of $YBa_2Cu_3O_7$. Since this material has significant carrier concentration, even in the normal state we have used both screened and unscreened versions of the shell model. The screened model gives a better overall description of the lattice dynamics of $YBa_2Cu_3O_7$. The phonon dispersion curves along the symmetry directions and the weighted phonon density of states for both $YBa_2Cu_3O_6$ and $YBa_2Cu_3O_7$ are presented.

1. Introduction

The lattice dynamics of $YBa_2Cu_3O_{6+x}$ has been extensively studied since the discovery of high temperature superconductivity in the highly oxygenated phase ($0{\cdot}5 \leq x < 1$). In conventional superconductors the vital role played by phonons is well established. However, in the high T_c superconductors the role of phonons is controversial. Even if they do not mediate the pairing mechanism, they are likely to play an important subsidiary role (Cardona 1989), hence the on-going interest in the phonon structure of these materials.

Experimental information on the phonon frequencies is obtainable from infrared absorption and Raman spectroscopy, which probe the $\boldsymbol{q} = 0$ modes, and from inelastic neutron scattering which allows one to measure the phonon dispersion curves throughout the Brillouin zone. A recent Raman study on a twin-free crystal of O_7 material has been reported by McCarty *et al.* (1990). Genzel *et al.* (1989) have reported infrared reflectivity measurements for $O_{6{\cdot}86}$. The early experiments using neutrons concentrated mainly on determination of the phonon density of states (Renker *et al.* 1988*a*, 1988*b*; Rhyne *et al.* 1987). A review by Feile (1989) cites most of the early work in this area.

A significant recent development on the experimental side has been the single crystal neutron work of the group in Karlsruhe (Reichardt *et al.* 1989*a*, 1989*b*; Reichardt 1990; Pyka *et al.* 1990; Rietschel *et al.* 1989; Pintschovius 1990). This work has, for the first time, provided precise knowledge of many phonon branches in all the symmetry directions for both $YBa_2Cu_2O_6$ and $YBa_2Cu_3O_7$. It has thus become meaningful to attempt to determine the parameters of lattice dynamical

0004-9506/92/020221$05.00

models by a least squares fit to the experimental data, a procedure which is well established and highly successful for simpler materials.

Existing lattice dynamical calculations for $YBa_2Cu_3O_{6+x}$ ($x = 0, 1$) have used three types of models. Bates (1989) and others have used a valence-bond force model, based on bond-stretching and bond-bending coordinates. Such a model has the advantage of being well adapted to describe covalent bonding but neglects the ionic Coulomb interactions. This work considered only the $\boldsymbol{q} = 0$ modes. Rigid ion models have been developed by many authors (Chaplot 1988; Bruesch and Buhrer 1988; Qin and Jiang 1989; Belosludov *et al.* 1989). These calculations neglect the polarisability of the ions, which is clearly important in these materials. The shell model has been proposed to overcome this deficiency and has been extremely successful for simpler materials, including highly covalent materials. Comprehensive shell model calculations for the O_7 material, using model parameters obtained from calculations on other materials with the same ionic configuration, have been carried out by Kress *et al.* (1988) who obtained good agreement with experimental $\boldsymbol{q} = 0$ frequencies.

In the present work we have developed a shell model description for $YBa_2Cu_3O_{6+x}$ ($x = 0, 1$) in which the shell model parameters are determined by a least squares fit to the experimental phonon dispersion curves measured by the Karlsruhe group. The parameter values obtained in this way are more appropriate and yield a better overall fit than the values used by Kress *et al.* (1988). For the O_6 material we have considered two models, to be described in the following section. For the O_7 material the question of screening of the Coulomb interactions is important, as this material has a significant density of free carriers. We have considered both unscreened and screened models, as described below. Similar calculations have been reported by the Karlsruhe group (Pyka *et al.* 1990), but few details of their calculations have been given.

2. Theory

The shell model is a phenomenological model which incorporates short-range forces, long-range Coulomb forces and electronic and short-range polarisabilities of ions in the crystal. The polarisability of an ion is modelled by assuming that the ion consists of a core and a shell, with the core coupled to its shell by a spring of force constant k. Both the core and the shell carry charges but only the core has a nonzero mass. On the assumption that the short-range forces act through the shells only, the equations of motion can be written (in matrix–vector notation) as

$$\begin{aligned} \omega^2 \boldsymbol{M}\boldsymbol{u} &= (\boldsymbol{R} + \boldsymbol{ZCZ})\boldsymbol{u} + (\boldsymbol{R} + \boldsymbol{ZCY})\boldsymbol{w}\,, \\ 0 &= (\boldsymbol{R}^{+} + \boldsymbol{YCZ})\boldsymbol{u} + (\boldsymbol{R} + \boldsymbol{k} + \boldsymbol{YCY})\boldsymbol{w}\,. \end{aligned}$$

Elimination of $\boldsymbol{w}$ yields

$$\begin{aligned} \omega^2 \boldsymbol{M}\boldsymbol{u} = [&(\boldsymbol{R} + \boldsymbol{ZCZ}) - (\boldsymbol{R} + \boldsymbol{ZCY}) \\ &\times (\boldsymbol{R} + \boldsymbol{k} + \boldsymbol{YCY})^{-1}(\boldsymbol{R}^{+} + \boldsymbol{YCZ})]\boldsymbol{u}\,. \end{aligned}$$

Here $\boldsymbol{Z}$, $\boldsymbol{Y}$, $\boldsymbol{k}$ and $\boldsymbol{M}$ are diagonal matrices of the charges on the ions, the charges on the shells, the core–shell spring constants and the ionic masses respectively. The vector $\boldsymbol{u}$ is the displacement of cores from their equilibrium positions and $\boldsymbol{w}$ the displacement of the shells from their cores. It should be pointed out that the Coulomb matrix $\boldsymbol{C}$ in the $\boldsymbol{YCY}$ term differs from the rest of the Coulomb matrices by a constant (Traylor *et al.* 1971). The matrix $\boldsymbol{R}$ is the short-range force constant matrix. We approximate the short-range forces between an ion pair by a two-body axial symmetric force:

$$\phi^{\mathrm{R}}_{\alpha\beta}(r) = -\frac{e^2}{2v_{\mathrm{a}}}\left((A-B)\frac{r_\alpha r_\beta}{r^2} + \delta_{\alpha\beta}B\right),$$

where e is the electronic charge, r the bond length, v_{a} the volume of the unit cell, and A and B the radial and tangential force constants.

Screening: When screening is taken into consideration the bare Coulomb potential is replaced by $\phi^{\mathrm{C}} = \mathrm{e}^{-\alpha r}/r$, where α is the inverse of the screening length. This additional exponential factor in the potential affects all of the Coulomb coefficients in the shell model. This is because free carriers would screen electric fields from every source in the crystal, be it electric fields of the ion cores or the electron shells, as suggested by Cowley *et al.* (1969). This approach is rather different from that described by Weber (1973) for the calculation of phonon frequencies for some transition metal carbides with superconducting properties.

An explicit form for the correction to the unscreened Coulomb coefficients due to screening was given by Cowley *et al.* (1969). The correction terms contain a number of extra parameters and, further, they converge rather slowly. Hence, instead of using their formulation we performed an Ewald transformation on the screened Coulomb potential, as described but not implemented by Cowley *et al.* (1969). The resulting expressions contain non-standard integrals which have to be evaluated numerically but, since they are independent of $\boldsymbol{q}$, they are calculated once and stored. As a result the calculations with screening are not computationally more demanding than those without screening which involve the standard Ewald transformation.

Phonon Density of States: The phonon density of states is defined by

$$G(E) = \sum_{q,j} \delta\big(E - E(\boldsymbol{q}, j)\big)\,.$$

However, experimental measurements do not give this quantity but rather a weighted density of states which has the form (Lustig *et al.* 1985)

$$G(E) = \mathrm{const} * \sum_{q,j}\sum_{i}^{n} \frac{b_i^2}{2m_i}\langle[\boldsymbol{Q}\,.\,\boldsymbol{e}_i(\boldsymbol{q}, j)]^2 \mathrm{e}^{-2w_i}\rangle \delta\big(E - E(\boldsymbol{q}, j)\big)\,.$$

The summation i is over all n atoms in the unit cell and j is over all $3n$ branches with wavevector $\boldsymbol{q}$. Here b_i and m_i are the scattering length and the mass of the ith atom in the unit cell, while $\boldsymbol{e}_i(\boldsymbol{q},j)$ is the eigenvector of the ith atom in the $(\boldsymbol{q},j)$ mode. In our calculation the contributions from the Debye–Waller factors

w_i are assumed to be constant and hence ignored. Further, $\boldsymbol{Q}$ is a unit vector in the direction of momentum transfer which is taken to be in the range 6–10 Å^{-1}. We find that although minor features of the density of states are sensitive to the range of momentum transfer, its general features are largely unaffected. In using this formula only the one-phonon contribution to the phonon density of states is included.

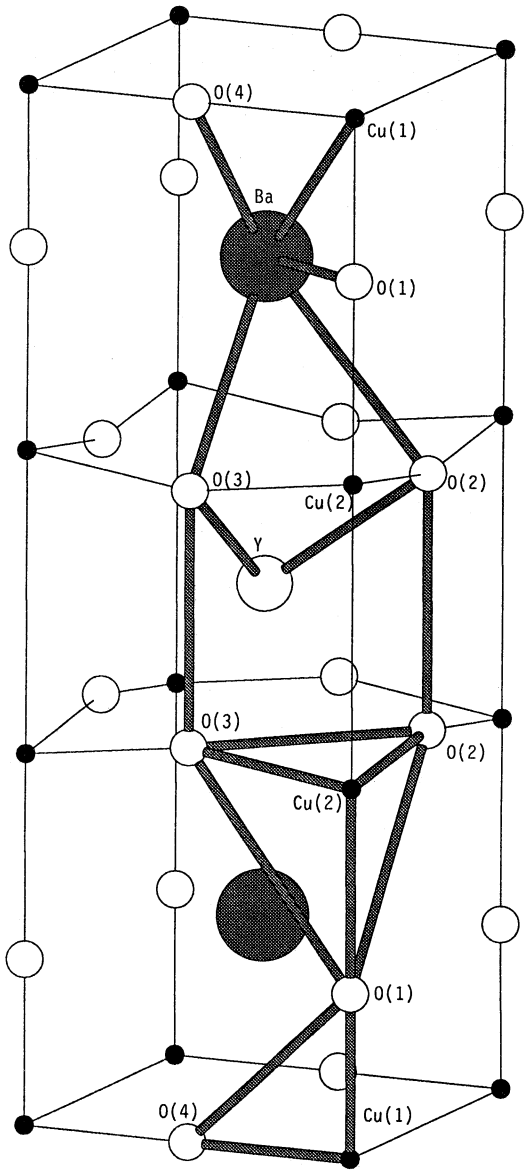

Fig. 1. Conventional unit cell of $YBa_2Cu_3O_7$ and the labelling of ions. The thick lines show the short-range interactions which we have used. In $YBa_2Cu_3O_6$ the oxygen O(4) is missing; no short-range interactions involving O(4) are included.

Table 1. Shell model parameters of Models 1 and 2 of $YBa_2Cu_3O_6$

The uncertainties quoted are obtained in the usual way from the least squares fitting procedure. The two results for k_x, k_y for the O(2,3) ions, denoted a and b (in columns 4 and 8), represent the core–shell spring constants perpendicular and parallel to the Cu–O–Cu bond

Ion pair	Model 1 Short-range force constants A	Model 1 Short-range force constants B ($e^2/2v_a$)	Model 1 Uncertainty A	Model 1 Uncertainty B	Model 2 Short-range force constants A	Model 2 Short-range force constants B ($e^2/2v_a$)	Model 2 Uncertainty A	Model 2 Uncertainty B
Y–O(2,3)	297·66	−55·25	7	4	176·23	−27·49	11	4
Ba–O(1)	72·01	−6·56	3	2	53·91	−18·16	5	2
Ba–O(2,3)	67·67	9·15	6	3	68·79	11·60	8	3
Cu(1)–O(1)	790·93	−37·99	180	7	586·54	46·65	76	5
Cu(2)–O(1)	107·22	4·09	9	9	56·78	12·39	8	6
Cu(2)–O(2,3)	518·50	−50·50	13	5	402·02	−24·69	24	5
O(1)–O(2,3)	−10·04	−11·08	5	2	−5·54	−9·65	3	1·5
O(2,3)–O(3,2) (planar)	−32·69	1·23	8	1·5	−14·11	−0·76	6	1·5
O(2/3)–O(2/3) (vertical)	8·15	−10·20	4	3	19·32	−7·63	3	2
Ba–Cu(1)	3·03	8·30	5	3	26·28	8·87	5	2

Ion	Ionic charge (e)	Shell charge (e)	$k_x(k_y)$ (e^2/v_a)	k_z (e^2/v_a)	Ionic charge (e)	Shell charge (e)	$k_x(k_y)$ (e^2/v_a)	$k_z(e^2/v_a)$
Y	2·8	0·852±0·3	619±120	1343±280	1·934±0·1	−4·742±0·5	5520±710	10000
Ba	1·5	2·982±0·3	698±250	337±80	1·422±0·1	2·423±0·3	298±90	640±330
Cu(1)	1·5	4·485±1·3	10000	10000	0·600	5·833±0·7	10000	10000
Cu(2)	1·9	2·417±0·1	575±80	551±140	1·576±0·1	2·435±0·1	950±180	1590±910
O(1)	−1·85	−3·243±0·2	496±60	212±90	−1·196±0·1	−3·626±0·4	3850±3300	550±160
O(2,3)	−1·85	−3·061±0·2	a 1440±210	598±80	−1·534	−3·171±0·3	a 4160±1330	840±160
			b 1110±220				b 2030±490	

3. Results

(3a) $YBa_2Cu_3O_6$

We first discuss our results for $YBa_2Cu_3O_6$, for which the most detailed experimental results are available. The lattice structure is taken from Renker *et al.* (1988*b*). Initial shell model parameters are taken from the calculations of Kress *et al.* (1988) for $YBa_2Cu_3O_7$, with minor modifications. These are then varied in a least squares procedure to obtain an optimum fit to the Karlsruhe group's experimental phonon data.

Initially, for Model 1, the ionic charges are held fixed at values close to the nominal ones, preserving overall charge neutrality. The ionic charges of all the oxygen atoms are assumed to be the same, but the ionic charges of Cu(1) and Cu(2) are different, reflecting the different bonding environment of each. Similar results have been used by Chaplot (1990) in his rigid ion model. The short-range interactions used in our models are shown in Fig. 1, which also shows the structure and the labelling of atoms in the unit cell. This set of short-range interactions is essentially the same set used by Kress *et al.* (1988) for $YBa_2Cu_3O_7$, but to obtain a better fit we found it necessary to also include the Ba–Cu(1) interaction. The shell charges are allowed to take either negative or positive values, the latter being reasonable when a metal ion is surrounded by larger negative ions, as in the overlap shell model (Bilz *et al.* 1975). Anisotropic polarisabilities are assumed and hence for every ion there are two core–shell spring constants k_x, k_z. All the parameters in Model 1, except the ionic charges of all the ions and the k values of Cu(1), are allowed to vary freely. In Model 2 the ionic charges are allowed to vary as well, but that of Cu(1) is held fixed after it was reduced to 0·6, a value used by Chaplot (1990). In this model it is also necessary to fix k_z of Y in addition to the spring constants of Cu(1). These k values are constrained to a maximum value of 10 000 e^2/v_a, as otherwise we found that they would increase indefinitely. The maximum value is immaterial as any k large enough would imply an essentially unpolarisable ion. Model 2 gives a somewhat better overall fit ($\Delta f \approx 6\ \mathrm{cm}^{-1}$) compared with Model 1 ($\Delta f \approx 8\ \mathrm{cm}^{-1}$). Here Δf represents the root-mean-square deviation

$$\Delta f^2 = \frac{1}{N}\sum (f_{\mathrm{expt}} - f_{\mathrm{calc}})^2 .$$

The values of the shell model parameters used for Model 1 and Model 2 are shown in Table 1. In Fig. 2 we show the dispersion curves for both Model 1 and Model 2, for the $[\zeta 00/0\zeta 0]$ direction. The experimental results of the Karlsruhe group are shown for comparison. Similar results for the $[\zeta\zeta 0]$ and $[00\zeta]$ directions are shown in Figs 3 and 4 respectively. The weighted phonon density of states $G(E)$ for both models and the experimental results (Renker *et al.* 1988*a*) are shown in Fig. 5. No smoothing function has been used.

(3b) $YBa_2Cu_3O_7$

We now turn to the superconducting material $YBa_2Cu_3O_7$. The structural parameters are taken from Beech *et al.* (1987) (their third set corresponding

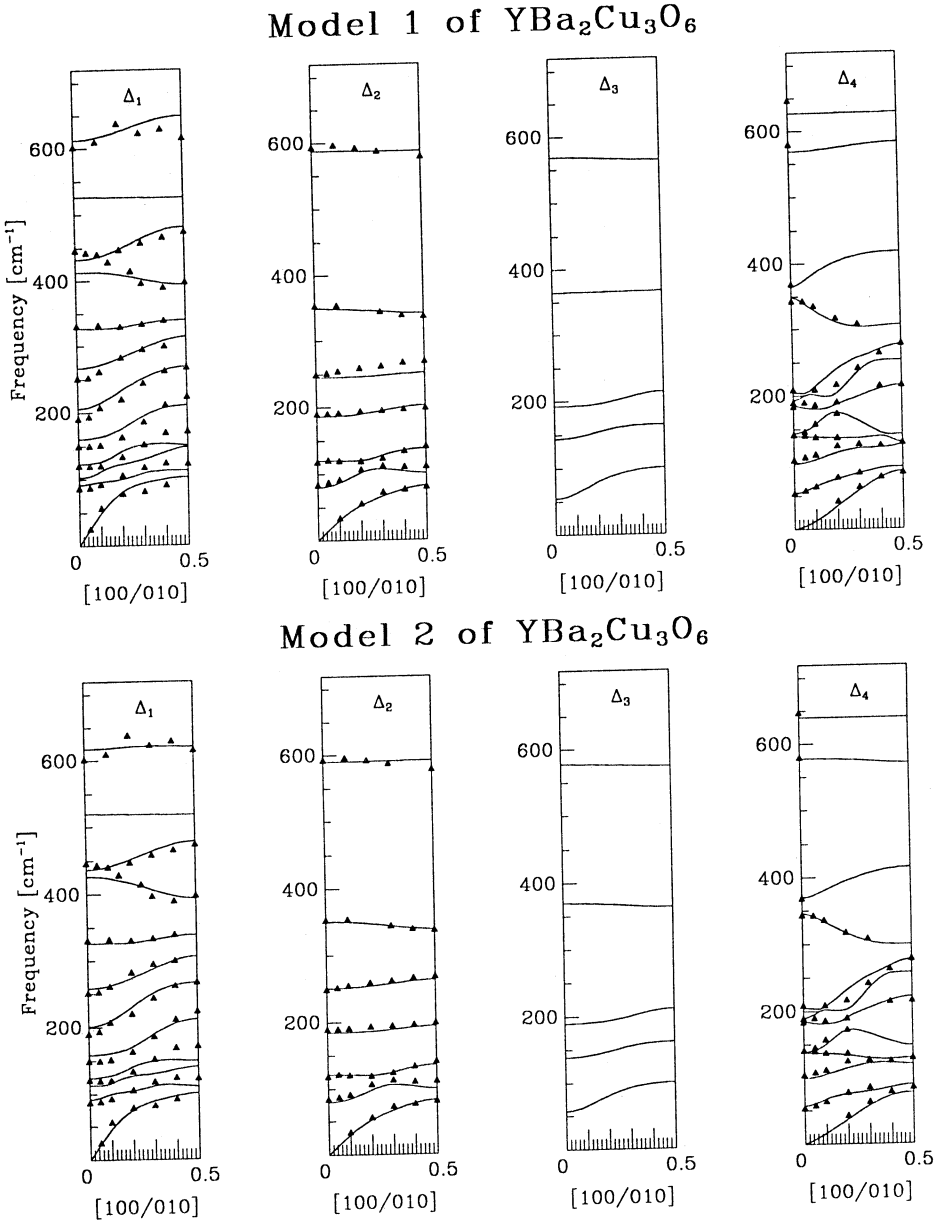

Fig. 2. Dispersion curves of $YBa_2Cu_3O_6$ in the [ζ00/0ζ0] direction. The experimental points (triangles) of the Karlsruhe group are plotted for comparison.

to an annealed sample at room temperature). We assume the orthorhombic structure, in which the oxygen atoms in the CuO plane are completely ordered into chains, ignoring the fact that twinning is possible in a real crystal.

The existing experimental data on this material are not complete enough for a detailed least squares fitting procedure. We have therefore proceeded by

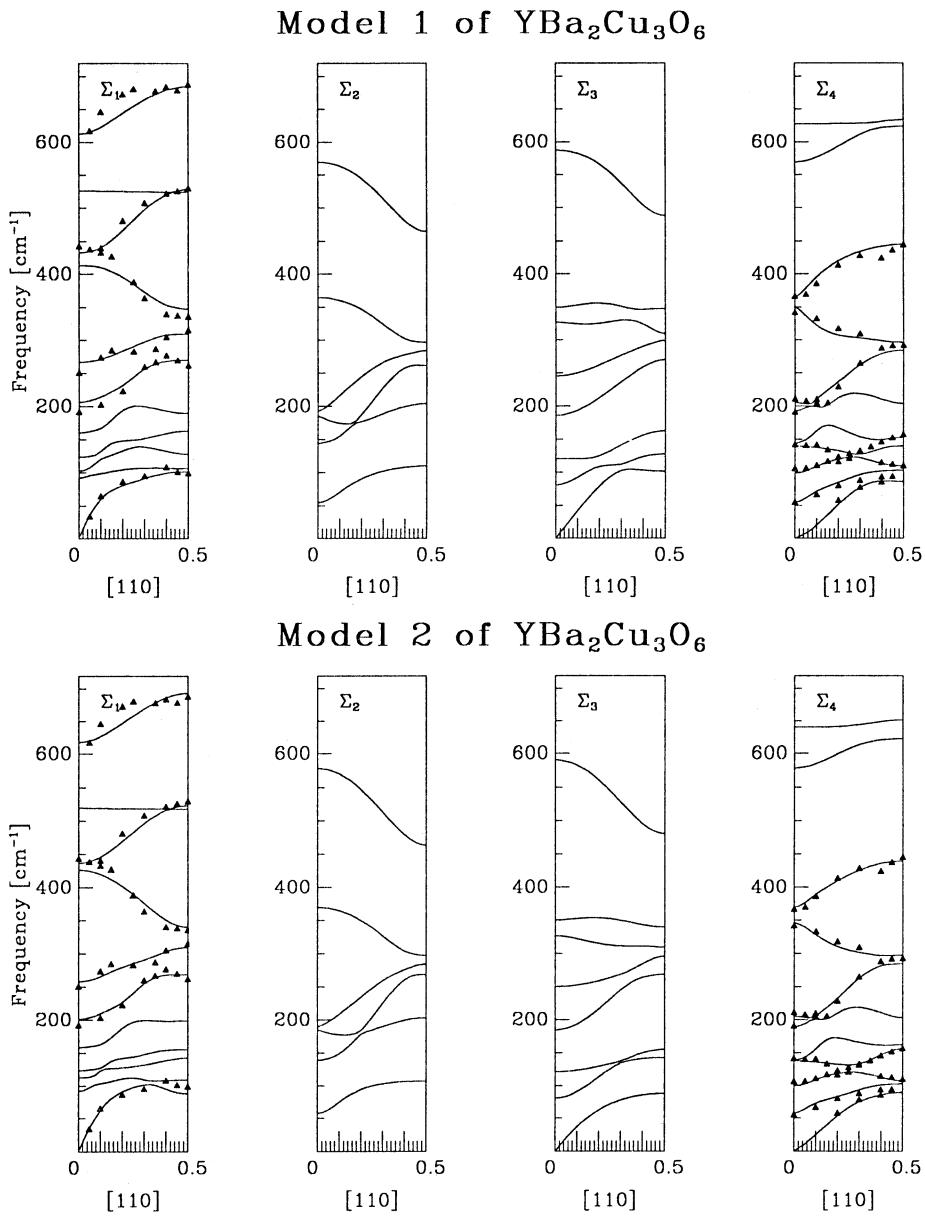

Fig. 3. Dispersion curves of $YBa_2Cu_3O_6$ in the [ζζ0] direction. The experimental points (triangles) of the Karlsruhe group are plotted for comparison.

taking as an initial parameter set that of our Model 1 for the O_6 material. The parameter set from Model 1 of O_6 is used rather than that of Model 2 because the ionic charges are near their nominal values and it contains fewer parameters, allowing a better interpretation of the model. The shell charge and spring constants of the extra oxygen O(4) are taken to be the same as for O(1), since these two ions have similar environments. The ionic charges of Cu(1) and

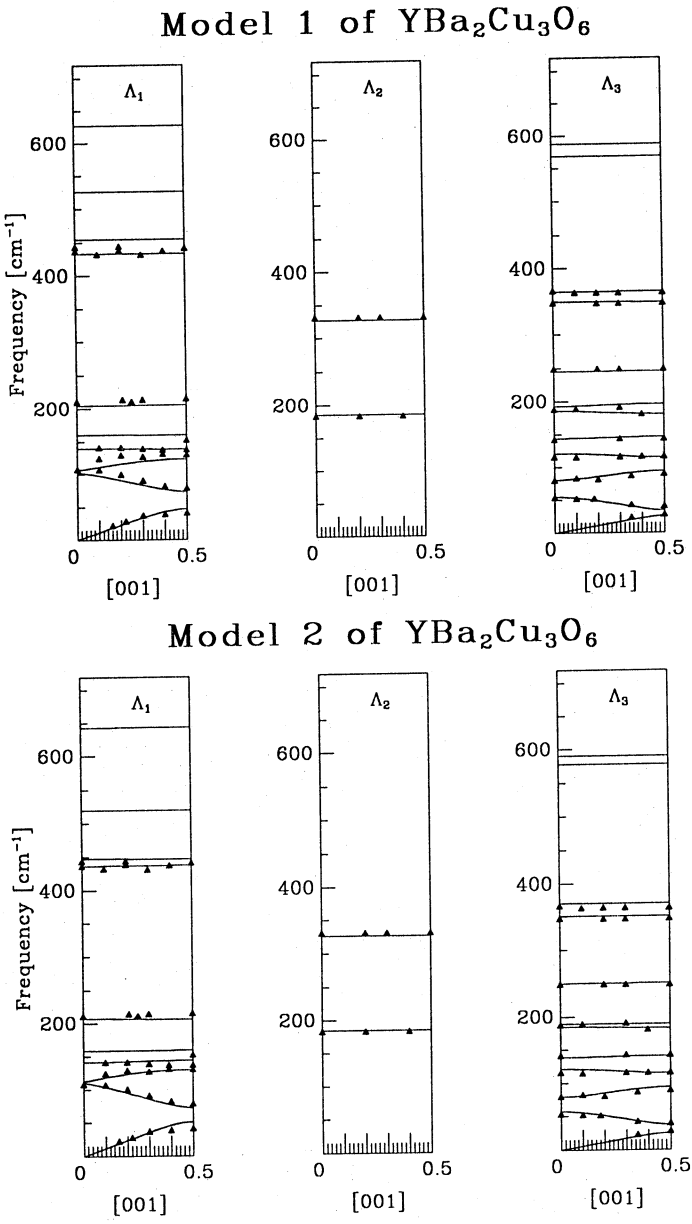

Fig. 4. Dispersion curves of $YBa_2Cu_3O_6$ in the $[00\zeta]$ direction. The experimental points (triangles) of the Karlsruhe group are plotted for comparison.

Ba are slightly increased to compensate for the inclusion of the O(4) oxygen. The radial and tangential short-range force constants in O_7 are obtained from O_6 using the assumption (Finlayson *et al.* 1986)

$$f_n = f_0 \left(\frac{R_0}{R_n} \right)^3 \frac{v_n}{v_0},$$

where R is the bond length of the ion pair and v is the volume of the unit cell. This formula is strictly valid only for Coulombic interactions but should be a reasonable approximation in other cases.

This initial parameter set was inadequate as dynamic instabilities were found in many regions of the Brillouin zone. By slight variations, particularly of the parameters involving the extra oxygen, we were able to obtain a parameter set for which there were no instabilities at any $\boldsymbol{q}$ and which gave a reasonable fit to the zone centre frequencies and to the available dispersion curves. We refer to this as Model 1 (of O_7).

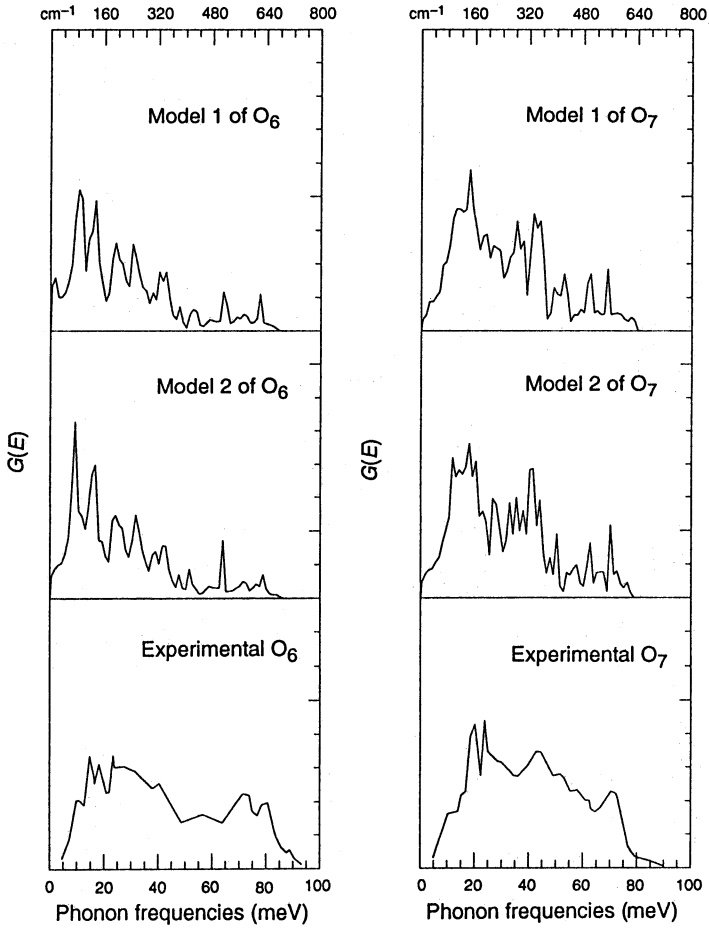

Fig. 5. Weighted one-photon density of states for $YBa_2Cu_3O_6$ and $YBa_2Cu_3O_7$. The experimental curves are those of Renker *et al.* (1988*a*).

Model 1 suffers from the deficiency that the Coulomb interactions are unscreened. In fact the O_7 material has a significant density of free carriers (Wang *et al.* 1987) and therefore screening might well be important and should be incorporated. This is done as discussed in Section 2. The screening length is an additional unknown parameter. We used the value 2 Å, one consistent with the screening

Table 2. Shell model parameters for $YBa_2Cu_3O_7$

The two results for k_x, k_y for O(2,3) ions, denoted by a and b, represent the planar core–shell spring constants perpendicular and parallel to the Cu–O–Cu plane. The screening length used in Model 2 is 2 Å. For Model 2 the parameters shown are those that differ from Model 1

Ion pair	Unscreened (Model 1)		Screened (Model 2)	
	A	B $(e^2/2v_a)$	A	B $(e^2/2v_a)$
Y–O(2)	290·7	−53·9		
Y–O(3)	299·6	−55·6		
Ba–O(1)	90·5	−6·0		
Ba–O(2)	61·7	8·3		
Ba–O(3)	63·2	8·5		
Ba–O(4)	68·0	−7·2		
Ba–Cu(1)	3·2	8·9		
Cu(1)–O(1)	710·0	−28·0		
Cu(1)–O(4)	350·0	−40·0		
Cu(2)–O(1)	135·0	1·9		−3·9
Cu(2)–O(2)	521·0	−50·8		
Cu(2)–O(3)	466·0	−48·3		
O(1)–O(2)	−10·8	−11·9		
O(1)–O(3)	−10·6	−11·7		
O(1)–O(4)	−5·5	4·0		1·0
O(2)–O(2)	8·1	−10·2		
O(3)–O(3)	8·0	−10·1		
O(2)–O(3) (planar)	−32·4	5·2		
Core–shell forces (e^2/v_a)				
Y	(619, 619, 1343)			
Ba	(699, 699, 337)			
Cu(1)	(2000, 2000, 2000)			
Cu(2)	(575, 575, 551)			
O(1)	(496, 496, 212)			
O(2,3) (a, b, z)	(1003, 1110, 598)			
O(4)	(496, 1003, 496)			
Ionic charges (e)	Y = 2·80	Ba = Cu(1) = 1·85		Cu(2) = 1·95
	O(1) = 1·70	O(2,3) = 1·80		O(4) = 1·65
Shell charges (e)	Y = 0·85	Ba = Cu(1) = 2·98		Cu(2) = 2·42
	O(1) = −2·74	O(2,3) = −3·06		O(4) = −2·74

length of a simple metal having the same carrier density. In any case the results are not very sensitive to the precise value of this parameter. Model 2 incorporates screening as well as minor changes in two other parameters.

The values of the model parameters used for $YBa_2Cu_3O_7$ are shown in Table 2, while Table 3 gives the experimental and calculated normal mode frequencies. Fig. 6 shows the dispersion curves for Model 1 and Model 2 for $\boldsymbol{q}$ in the $[\zeta 00]$ direction. Figs 7, 8 and 9 give the corresponding results for the $[0\zeta 0]$, $[00\zeta]$ and $[\zeta\zeta 0]$ directions respectively. Experimental results for the $[\zeta\zeta 0]$ and $[00\zeta]$ directions are shown for comparison. For other directions, the experimental results are affected by twinning, hence they are not presented for comparison. The phonon density of states is shown in Fig. 5.

4. Discussion and Conclusions

We have shown that it is possible, using a rather simple model, to obtain a fairly accurate overall representation of the lattice vibrations in these complex, highly

Table 3. Normal mode frequencies at $q = 0$ of $YBa_2Cu_3O_7$ (in cm^{-1})
For comparison the experimental results of McCarty *et al.* (1990) and Genzel *et al.* (1989) are shown

Screened			Unscreened			Experimental		
A_g	B_{2g}	B_{3g}	A_g	B_{2g}	B_{3g}	A_g	B_{2g}	B_{3g}
119	69	77	121	66	77	116	70	83
155	140	144	158	146	149	149	142	140
355	218	292	358	213	298	337	210	303
417	364	371	429	361	368	433		
501	569	537	501	565	532	500	579	526
B_{1u}	B_{2u}	B_{3u}	B_{1u}[A]	B_{2u}[A]	B_{3u}[A]	B_{1u}	B_{2u}	B_{3u}
100	88	68	77(99)	99(101)	68(77)			
166	165	86	166(182)	160(162)	99(100)	155		
199	191	166	212(213)	190(210)	148(150)	195		
274	301	185	267(267)	301(303)	183(210)	275		
318	351	271	321(356)	352(409)	282(288)	311		
366	477	340	391(452)	443(480)	344(423)			
566	550	581	564(564)	549(586)	581(603)	569		

[A] Tranverse optic and (in parentheses) longitudinal optic mode frequencies are given.

anisotropic materials. Nevertheless, a number of discrepancies remain indicating that either additional interactions or other features such as anharmonicity may be important. A general feature which we have observed, and which has also been noted by Kress *et al.* (1988), is the strong tendency towards dynamical instabilities, revealed by negative eigenvalues of the dynamical matrix. The windows in parameter space in which there is phonon stability throughout the zone appear to be very narrow.

$YBa_2Cu_3O_6$: We have considered two models, with the parameters obtained by a least squares fit to experimental phonon frequencies. Model 1, in which the ionic charges are held fixed, gives a reasonable overall fit with an average frequency deviation $\Delta f \approx 8\ cm^{-1}$. However, it can be seen from the dispersion curves that the fit worsens towards the zone boundary, particularly for those modes along the $[\zeta 00/0\zeta 0]$ direction. We found that in general those phonon modes which are polarised in the z direction are especially hard to fit. This indicates that more short-range forces, in particular those between ions in different layers along the z direction, may need to be included. The highest Δ_1 and Σ_1 modes, though not polarised in the z direction, are also hard to fit. These modes involve predominantly x, y motion of the basal plane oxygens O(2,3), suggesting some extra force terms among these oxygens might be necessary for their description.

Two types of instabilities are encountered in Model 1. One of the acoustic modes along the $[\zeta 00/0\zeta 0]$ direction tends to have a negative slope at the zone centre if the corresponding experimental acoustic branch is not heavily weighted in the fitting procedure. A similar type of instability was found in our calculations for $YBa_2Cu_4O_8$ (Yim *et al.* 1991). Near the point $(0{\cdot}12, 0{\cdot}12, 0{\cdot}5)$ there is also a very soft mode. Since there are no experimental data available for this mode we have fitted this mode to that of Model 2, which is dynamically stable. These two types of instabilities are ionic charge related as they could be eliminated by reducing the ionic charges in the Cu(1)–O(1)–Ba sublattice, and in particular

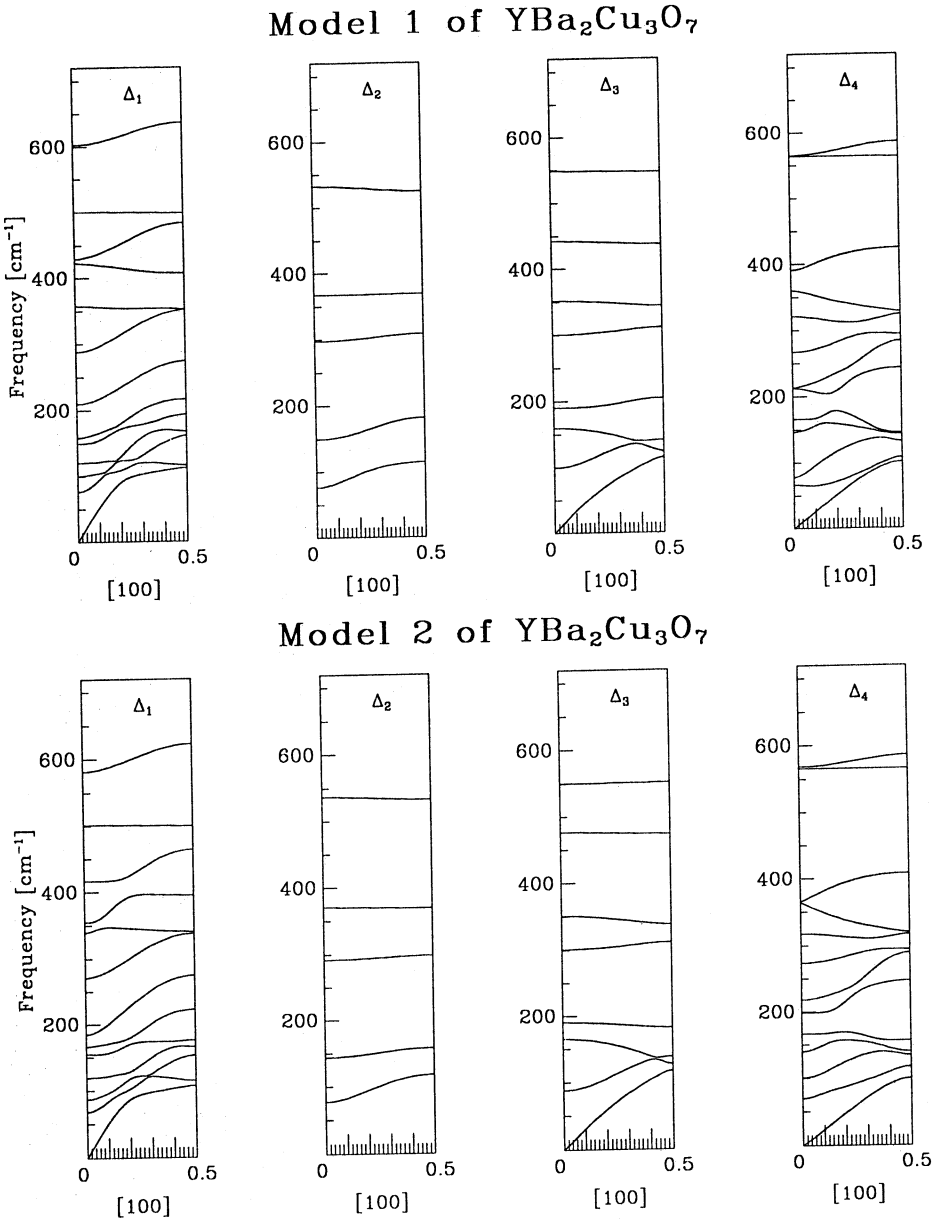

Fig. 6. Dispersion curves of $YBa_2Cu_3O_7$ in the $[\zeta 00]$ direction.

that of Cu(1). Hence, these pose no major problem to us in Model 2 in which the ionic charges have been included as least squares variables.

The phonon density of states obtained from both models is only in fair agreement with experiment. Many of the measured peaks are well produced by the models but the relative intensities of the peaks in our calculations differ from

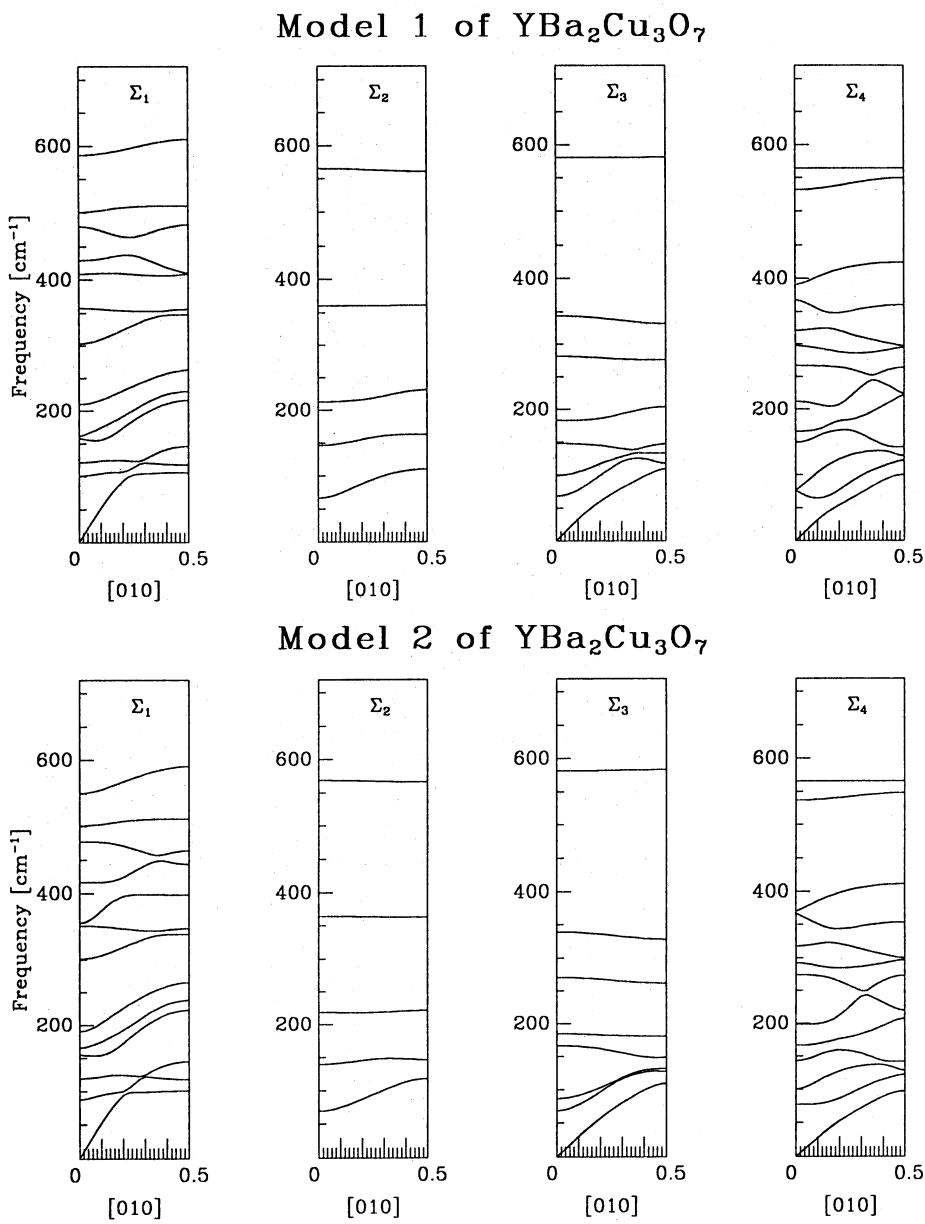

Fig. 7. Dispersion curves of $YBa_2Cu_3O_7$ in the $[0\zeta 0]$ direction.

the experimental ones. In particular, the first few peaks in the lower energy region of the spectrum are too intense while the intensity in the high energy region is far too weak. This high energy section is predominantly due to the vibrations of O(1) and O(2, 3). Another distinct discrepancy of the calculated phonon density of states is the peak at 65 meV which is not present in the experimental data.

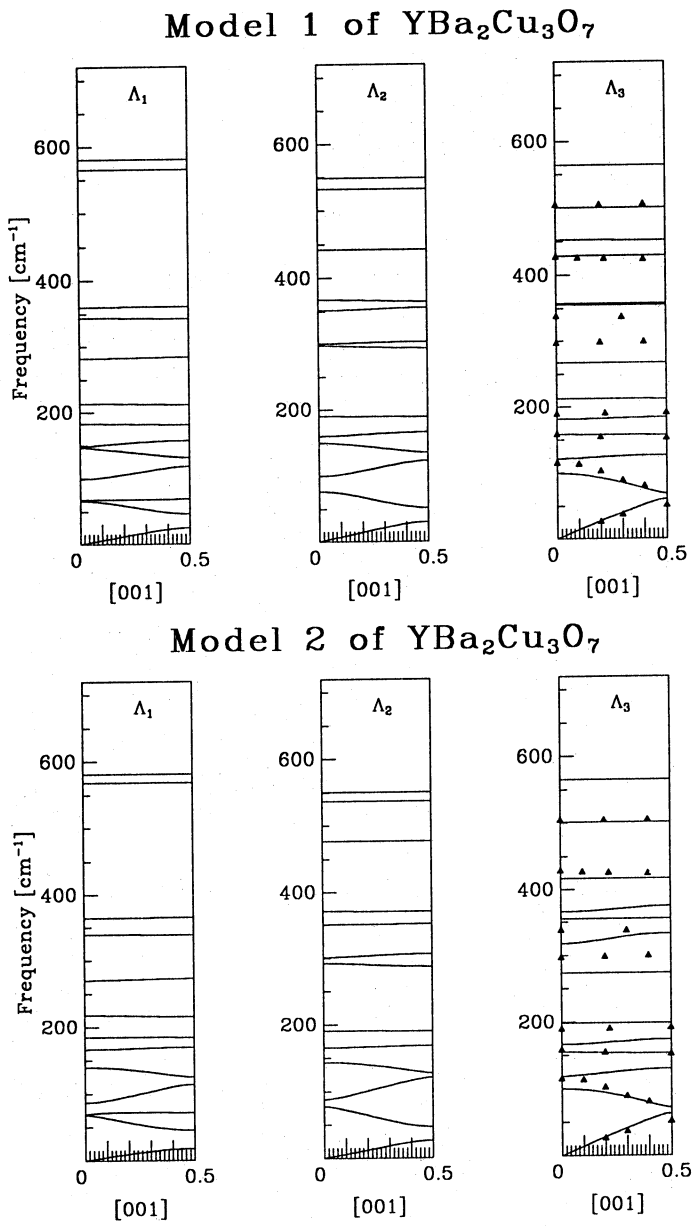

Fig. 8. Dispersion curves of $YBa_2Cu_3O_7$ in the [00ζ] direction. The experimental points (triangles) of the Karlsruhe group are plotted for comparison.

It is possible that this peak will shift to 70 meV if the additional model features mentioned above are included.

The parameter set obtained from the least squares fitting can give us much useful information. For a start the large uncertainties in the parameters reflect

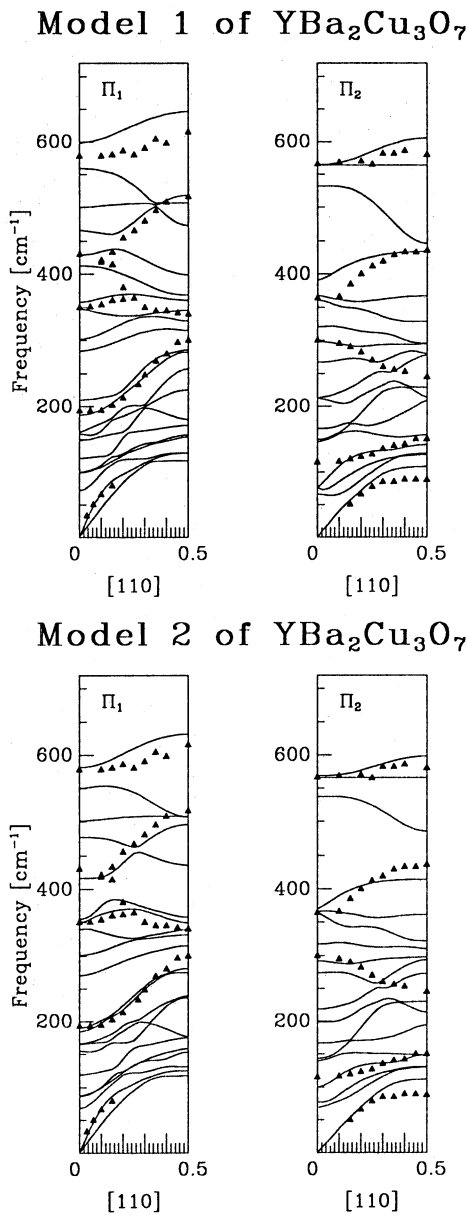

Fig. 9. Dispersion curves of $YBa_2Cu_3O_7$ in the [$\zeta\zeta$0] direction. The experimental points (triangles) of the Karlsruhe group are plotted for comparison.

the non-uniqueness of the parameter set. The inclusion of the ionic charges as least squares variables (Model 2) improves the fitting significantly ($\Delta f \approx 6$ cm^{-1}). The ionic charges obtained from the least squares routine are rather close to those used by Chaplot (1990) in his rigid ion model calculations. Some of the ionic

charges are very small in magnitude, relative to their nominal values, particularly those of Y, Cu(1) and O(1). This may indicate that the O_6 material is highly covalent.

In both models most of the metallic ions have positive shell charges. The shell charges of Y, Ba and Cu(2) are explainable in terms of the overlap shell model while that of Cu(1), which is not fully surrounded by negative ions, suggests that there must be some complicated interactions within the Cu(1)–O(1)–Ba sublattice. In Model 2 the shell charge of Y becomes negative because its ionic charge and those of its neighbours have been reduced, significantly lessening the degree of charge overlap while the shell charge of Cu(1) remains positive despite having a much smaller ionic charge.

The short-range force constants turn out to be very different from those of Kress *et al.* (1988). Most of our short-range force constants between metallic ions and oxygens are much smaller than theirs. They used a Born–Mayer potential to represent the short-range repulsive forces. Our short-range force constants are not derivable from such a potential. In our models the radial force constants between metallic ions and oxygens appear to be roughly inversely proportional to the bond lengths. This is not the case for the oxygen–oxygen interactions. As for the magnitude of these force constants, the radial force constant of Cu(1)–O(1) is extremely large, indicating a stiff bond, while that of Cu(2)–O(2,3), being the second largest, shows a rigid CuO_3 octahedron.

$YBa_2Cu_3O_7$: The fitting for $YBa_2Cu_3O_7$ in both models is reasonably good. It can be seen that the screened model (Model 2) is clearly better than the unscreened one (Model 1), as can be seen in Figs 8 and 9 and Table 3. This is particularly true for those normal modes which involve the TO–LO splitting and the dispersion curves associated with them. The agreement with experiment for the z-polarised modes, namely, the A_g modes and the B_{1u} modes, is not very good in either model (see Table 3 and Fig. 8). The calculated acoustic modes in the $[\zeta\zeta 0]$ and $[00\zeta]$ directions are too high in energy at the zone boundary. The phonon density of states for both models is satisfactory, apart from having too low an intensity in the high energy region.

Our calculations for O_7 are based on the shell model parameters of O_6. The parameters belonging to the Cu(1)–O(1)–Ba–O(4) subsystem and a few others involving the Cu(2)–O(2,3) plane are slightly modified to give better agreement with experiment. The adjustments to the parameters of the Cu(1)–O(1)–Ba–O(4) system can be justified by the inclusion of the additional O(4) ions, which would definitely alter the bonding within the system, but the adjustment to the parameters of the Cu(2)–O(2,3) plane can only point to the limitation of the models. Additions to the shell model as discussed earlier for the O_6 material may prove important.

In summary, we have shown that many of the lattice dynamical features of $YBa_2Cu_3O_6$ and $YBa_2Cu_3O_7$ can be described by the shell model. In the $YBa_2Cu_3O_6$ material there is a high degree of covalency in the bonding, while in $YBa_2Cu_3O_7$ screening is important in describing the phonon features of the material. Despite the comments made above it is important to stress that it may be misleading to interpret the force constant parameters obtained from the least squares fitting procedure too literally. Nevertheless, such models provide a useful representation of the overall lattice dynamics of these materials and a necessary

starting point for calculations of higher order effects, such as anharmonicity or electron–phonon interactions.

Acknowledgments

We thank Dr W. Reichardt of Kernforschungszentrum Karlsruhe for sending us many preprints on the work of his group. We would also like to thank Dr T. R. Finlayson of Monash University for useful discussion. One of us (KKY) acknowledges support from the Australian Government through an EMSS scholarship, and support from AINSE through an AINSE Studentship. This work is also partially supported by an ARC grant.

References

Bates, F. E. (1989). *Phys. Rev.* B **39**, 322.
Beech, F., Miraglia, S., Santoro, A., and Roth, R. S. (1987). *Phys. Rev.* B **35**, 8778.
Belosludov, V. R., Lavrentiev, M. Yu., and Syskin, S. A. (1989). *Int. J. Mod. Phys.* B **3**, 611.
Bilz, H., Buchanan, M., Fischer, K., Haberkorn, R., and Schroder, U. (1975). *Solid State Commun.* **16**, 1023.
Bruesch, P., and Buhrer, W. (1988). *Z. Phys.* B **70**, 1.
Cardona, M. (1989). Proc. Ultrasonics Int. 89 Conference, Madrid, July 1989.
Chaplot, S. L. (1988). *Phys. Rev.* B **37**, 7435.
Chaplot, S. L. (1990). *Phys. Rev.* B **42**, 2149.
Cowley, E. R., Darby, J. K., and Pawley, G. S. (1969). *J. Phys.* C **2**, 1916.
Feile, R. (1989). *Physica* C **159**, 1.
Finlayson, T. R., Reichardt, W., and Smith, H. G. (1986). *Phys. Rev.* B **33**, 2473.
Genzel, L., Wittlin, A., Bauer, M., Cardona, M., Schonherr, E., and Simon, A. (1989). *Phys. Rev.* B **40**, 2170.
Kress, W., Schroder, U., Prade, J., Kulkarni, A. D., and de Wette, F. W. (1988). *Phys. Rev.* B **38**, 2906.
Lustig, N., Lannin, J. S., Carpenter, J. M., and Hasegawa, R. (1985). *Phys. Rev.* B **32**, 2778.
McCarty, K. F., Liu, J. Z., Shelton, R. N., and Radousky, H. B. (1990). *Phys. Rev.* B **41**, 8792.
Pintschovius, L. (1990). *Festkorperprobleme (Adv. Solid State Phys.)* **30**, 183.
Pyka, N., Reichardt, W., Pintschovius, L., and Collin, G. (1990). Proc. Int. Seminar on Neutron Physics, Alushta USSR, Oct. 1990.
Qin, J., and Jiang, Y. (1989). *Int. J. Mod. Phys.* B **3**, 1277.
Reichardt, W. (1990). *Neutron News* **1**, 20.
Reichardt, W., Ewert, D., Gering, E., Gompf, F., Pintschovius, L., Renker, B., Collin, G., Dianoux, A. J., and Mutka, H. (1989*a*). *Physica* B **156–7**, 897.
Reichardt, W., Pyka, N., Pintschovius, L., Hennion, B., and Collin, G. (1989*b*). *Physica* C **162–4**, 464.
Renker, B., Gompf, F., Gering, E., Ewert, D., Rietschel, H., and Dianoux, A. J. (1988*a*). *Z. Phys.* B **73**, 309.
Renker, B., Gompf, F., Gering, E., Roth, G., Reichardt, W., Ewert, D., Rietschel, H., and Mutka, H. (1988*b*). *Z. Phys.* B **71**, 437.
Rhyne, J. J., Neumann, D. A., Gotaas, J. A., Beech, F., Toth, L., Lawrence, S., Wolf, S., Osofsky, M., and Gubser, D. U. (1987). *Phys. Rev.* B **36**, 2294.
Rietschel, H., Pintschovius, L., and Reichardt, W. (1989). *Physica* C **162–4**, 1705.
Traylor, J. G., Smith, H. G., Nicklow, R. M., and Wilkinson, M. K. (1971). *Phys. Rev.* B **3**, 3457.
Wang, Z. Z., Clayhold, J., Ong, N. P., Tarascon, J. M., Greene, L. H., McKinnon, W. R., and Hull, G. W. (1987). *Phys. Rev.* B **36**, 7222.
Weber, W. (1973). *Phys. Rev.* B **8**, 5082.
Yim, K. K., Oitmaa, J., and Elcombe, M. M. (1991). *Solid State Commun.* **77**, 385.

Manuscript received 7 February, accepted 1 April 1992